SF2A 2011
G. Alecian, K. Belkacem, R. Samadi and D. Valls-Gabaud (eds)

RESULTS FROM THE FIRST THREE YEARS OF OPERATION OF THE SUPERNOVA LEGACY SURVEY (SNLS)

C. Balland[1, 2] and the SNLS collaboration

Abstract. Type Ia supernovae (SNe Ia) currently provide the most direct evidence for an accelerating Universe and for the existence of an unknown dark energy driving the expansion. The Supernova Legacy Survey (SNLS) is a five-year project which has delivered around 500 high-redshift SNe Ia light curves and spectra in the redshift range $0.2 < z < 1.0$ in order to constrain the dark energy equation-of-state, w. The cosmological results obtained with the data of the first 3 years of the survey are presented.

Keywords: type Ia supernovae, cosmology, dark energy, SuperNova Legacy Survey

1 Cosmology with Type Ia supernovae

Type Ia supernovae (SNe Ia) are thought to be the result of the thermonuclear explosion of a carbon-oxygen white dwarf reaching the Chandrasekhar mass limit. Observationally, they are rare (roughly one per galaxy and per thousand years), very bright ($L \sim 10^{10} L_\odot$) and transient ($\sim$ 1 month) events. Cosmological tests based on measuring their luminosity distance, which encodes the history of the universal expansion, rely on the assumption that they are standard candles. If true, the comparison of their fluxes at different redshifts gives access to the ratio of their luminosity distances as a function of the cosmological parameters governing the expansion of the universe. Namely, for two SNe Ia at z_1 and z_2:

$$\frac{d_L(z_1)}{d_L(z_2)} = \left(\frac{\phi_2}{\phi_1}\right)^{1/2} = \mathcal{F}(z_1, z_2, \Omega_M, \Omega_X, w),$$

where d_L and ϕ are the luminosity distance and apparent flux of the supernovae. Ω_M and Ω_X are the matter and dark energy density parameters. $w = p/\rho$ is the equation-of-state parameter, where p and ρ are the pressure and density of dark energy.

SNe Ia are actually known for not being standard candles: a dispersion of $\sigma(L_{max}) \sim 40$ % in their absolute B-band luminosity at maximum light exists . However, two empirical correlations between their physical properties and brightness are used to standardize them. One of these two correlations relates the light curve shape – the so-called 'stretch' parameter s – to the absolute magnitude of a SN Ia: the brighter the supernova, the slower the decrease of its luminosity with time. The other correlation involves the color c of a supernova: brighter supernovae are also found bluer. The use of these empirically established 'brighter-slower' and 'brighter-bluer' relationships allows one to reduce $\sigma(L_{max})$ to 15 %, leading to a 5% precision in distance measurements (Guy et al. 2010). Distance and redshift measurements of a large number of SNe Ia are used to build a redshift-distance (Hubble) diagram over a large redshift range. Combined with other probes, this diagram is used to constrain the equation-of-state of the dark energy (e.g., Astier et al. 2006; Kowalski et al. 2008; Kessler et al. 2009; Sullivan et al. 2011).

[1] LPNHE, 4 place Jussieu, 75252 Paris Cedex 05, France
[2] Université Paris 11, Orsay, F-91405, France
email: balland@lpnhe.in2p3.fr

2 The SNLS survey

The Supernova Legacy Survey (SNLS) is a five year french-canadian program than ran from 2003 to 2008, dedicated to the measurement of distant ($0.2 < z < 1.0$) SNe Ia light curves and spectra. It consisted in an imaging survey on the Canada France Hawaii telescope (CFHT) as part of the deep component of the CFHT-Legacy Survey, and a spectroscopic survey on 8/10-m diameter telescopes.

The SNLS imaging survey was a 5 year "rolling search" using MEGACAM at the prime focus of the CFHT. Each lunar month ($\sim$ 18 nights), repeated observations (every 3 to 4 nights) of two 1 square degree fields (out of the 4 fields of the CFHT-LS Deep survey) were performed in 4+1 filters ($griz+u$) for as long as the fields stayed visible (i.e., $\sim$ 6 months). With this technique, about 500 SNe Ia were observed and spectroscopically confirmed between 2003 and 2008, with early, pre-discovery SN photometry, leading to well sampled and measured light curves.

The SNLS spectroscopic survey primarily aimed at identifying the type of the SN and determining its redshift. It has also permitted detailed studies in the UV and optical part of SN spectra (e.g., Ellis et al. 2008; Sullivan et al. 2009; Balland et al. 2009). Spectra have been obtained at the VLT (during two large programs in service observing mode for a total of 480 hours of spectroscopy time between 2003 and 2007), at Gemini North and South (60 hours per semester) and Keck (30 hours during one semester).

3 Implementing the cosmological test

In SNLS, we have set up two independent analysis pipelines (one in France, one in Canada) for the photometric calibration, the SN photometry, the light curve fitters and the spectroscopic identification. Extensive comparisons between the two analyses allowed us to select at each step the most performant approach. When no objective reason for selecting one approach over the other was found, the differences were accounted for as systematics in our analysis. The uncertainties (both statistical and systematics) are included in the SNLS cosmological fits as a full variance-covariance matrix (available to the community; Conley et al. 2011). We describe the key ingredients of our analysis in the following.

3.1 Photometric and SN flux calibration

The SNLS 3 year analysis has led to a precise control of focal plane non-uniformities. Dithered observations of dense stellar fields have permitted to solve the non uniformities of the instrumental response. Variations in the instrumental response up to 8% difference along the focal plane and up to 4 nm in the effective wavelength of filters have been found and corrected for (Regnault et al. 2009).

A key feature of our cosmological test is that it relies on the comparison of low redshift SNe Ia with the high redshift homogenous sample of SNLS SNe Ia. Nearby SNe Ia are usually calibrated against the Landolt UBVRI system. To avoid introducing additional systematic uncertainties between distant and nearby SN fluxes, SNLS supernovae are also calibrated against Landolt stars. Color-color diagrams are used to translate Landolt UBVRI colors into MEGACAM $griz$ colors using piece-wise linear transformations. To obtain ratios of distances of SNe at low and high redshift, the ratio of fluxes of a reference star spectrum used as a calibrator is needed. For this purpose, we use BD+17^o 4708 as its colors fall in the same range as our observations of Landolt stars so that no extrapolation in colour-colour diagrams are required. This significantly reduces the systematic uncertainty associated with flux calibration compared to the 1st year analysis that relied on Vega colors (Regnault et al. 2009).

3.2 Light curve fitter and distance estimate

To measure the flux ratio of SNe at different redshifts in the same wavelength range and at the same phase*, it is necessary to interpolate light curve measurements obtained in different rest-frame bands with various time sampling. We use an empirical model of the SNe Ia spectral sequence that takes into account the diversity of SNe Ia via three parameters: a global luminosity offset x_0, a single shape parameter x_1 (related to the stretch s) and a global colour c. As an empirical model of the SNe Ia spectral sequence $\phi(SN, \phi, \lambda)$, we use SALT2 (Guy et al. 2007):

$$\phi(SN, \varphi, \lambda) = x_0[M_0(\varphi, \lambda) + x_1 M_1(\varphi, \lambda) + ...] \times \exp[c.CL(\lambda)]. \tag{3.1}$$

*The phase φ is the number of rest-frame days elapsed since B-band maximum light.

$CL(\lambda)$ is a colour variation law and $\{M_i\}$ is a set of linear principal components. Note that the color law does not assume any specific reddening by dust or intrinsic color variation. In particular, it does not follow a Cardelli extinction law. This model is trained both on nearby and distant (SNLS) SNe Ia. Using SNLS SNe Ia in the training process allows us to constrain the bluer part of the rest-frame spectrum without using observer frame U-band photometry, which is noticeably difficult to calibrate. The regular redshift sampling yields an accurate photometric scan of the SNe Ia spectra. Note that the light curve fit performed with this model is independent of any distance estimate.

As a distance estimate, we use the rest-frame B-band distance modulus μ_B:

$$\mu_B(z, \Omega_M, \Omega_X, w) = m_B - [M_B - \alpha.(s-1) + \beta.c],$$

with m_B the apparent peak magnitude in rest-frame B-band and M_B the absolute B-band peak magnitude for a "standard" SN Ia ($s = 1$; $c = 0$). The terms $\alpha.(s-1)$ and $\beta.c$ represent the way we implement the light curve shape and color corrections. β accounts for host galaxy dust extinction as well as for any intrinsic color property of SNe Ia. M_B, α and β are empirical coefficients fitted along with cosmology.

3.3 Environmental dependance of supernova properties

When one splits SNe Ia samples according to supernova host properties (host color, star formation rate, luminosity, stellar mass ...), differences in shape are found (Sullivan et al. 2006). The shape parameter is found larger in blue, highly star forming, less massive and fainter hosts: SNe Ia are brighter in these galaxies. However, after correction for the brighter-slower correlation, SNe Ia are found brighter in massive, early-type hosts (Sullivan et al. 2010). We perform an improved cosmological analysis by taking this effect into account. We consider two M_B parameters to be fitted along with the cosmological parameters: one for high-mass galaxies, and one for low-mass galaxies, with a split mass of $10^{10} M_\odot$ separating the two groups (Sullivan et al. 2011).

3.4 Spectroscopic identification

VLT spectra of the SNLS 3 year SNe Ia were analyzed with an optimized spectral extraction based on the use of the photometric profile of the host galaxy measured on deep stacked reference images as a model of the underlying galaxy. With this technique, host separation is very efficient in about 75% of cases (Baumont et al. 2008). In the remaining cases, no separate extraction of the SN and the host is attempted.

To identify the SN type, a simultaneous fit of the SN light curve and spectrum using SALT2 has been performed. A host component is added to the SALT2 SN Ia model and the best-fit host contribution to the full spectrum is obtained by χ^2 minimization. This procedure allows us to separate the host from the supernova component at the stage of identification in the spectra for which no separate extraction was possible.

4 Latest cosmological results from the SNLS

4.1 SNe Ia only constraints

The left panel of Fig. 1 presents an up-to-date Hubble diagram of SNe Ia from Conley et al. (2011). It compiles 242 SNLS, 123 nearby ($z \sim 0.05$), 93 SDSS-II ($z = 0.1 - 0.4$) and 14 HST ($z = 0.7 - 1.4$) SNe Ia, for a total of 472 SNe Ia. The regular sampling of data with redshift shows that the former gap at intermediate redshift has now been filled. The best-fit cosmological model and residuals are also plotted (see Conley et al. 2011 for details). Using SNe Ia alone, the universal acceleration is detected at the level of more than 99,9 %, including systematic effects. Assuming a flat universe, our results are consistent with the dark energy being a cosmological constant. Under this assumption, we find that $\Omega_M = 0.18 \pm 0.1$, $w = -0.91^{+0.17}_{-0.24}$ (syst. + stat). Assuming $\Omega_M = 0.27$, we obtain $w = -1.08 \pm 0.1$ (syst. + stat.). Including systematic uncertainties almost double the area of the confidence ellipses in the parameter planes under investigation. 97% of the systematics originate from calibration uncertainties, despite the considerable effort put in obtaining better than 1% accuracy on fluxes (Regnault et al. 2009). Uncertainties in the host split relationship and Malmquist bias come far behind as the second sources of systematics: each contributes 0,6% of the total systematic budget.

4.2 Using SNe Ia with other probes

Supplementing the supernova data with external probes such as baryon acoustic oscillations (BAO/DR7) and WMAP7, we find that the data are again consistent with the dark energy being a cosmological constant (Sullivan et al. 2011). Contours in the $w-\Omega_M$ plane are shown in the right panel of Fig. 1. Assuming flatness, we find $w = -1.061 \pm 0.069$ (a 6.5% measurement of the dark energy equation-of-state parameter) and $\Omega_M = 0.269 \pm 0.015$. Relaxing the flatness hypothesis, we find $w = -1.069 \pm 0.091$; $\Omega_M = 0.271 \pm 0.015$ and $\Omega_k = -0.002 \pm 0.006$ (Ω_k is the curvature density). The total error increases up to 9% in this latter case. Parameterizing the time evolution of w as $w(a) = w_0 + w_a(1-a)$, where a is the scale factor of the universe, gives $w_0 = -0.905 \pm 0.196$, $w_a = -0.984^{+1.094}_{-1.097}$ in a flat universe. Clearly, our data do not constrain the time evolution of w.

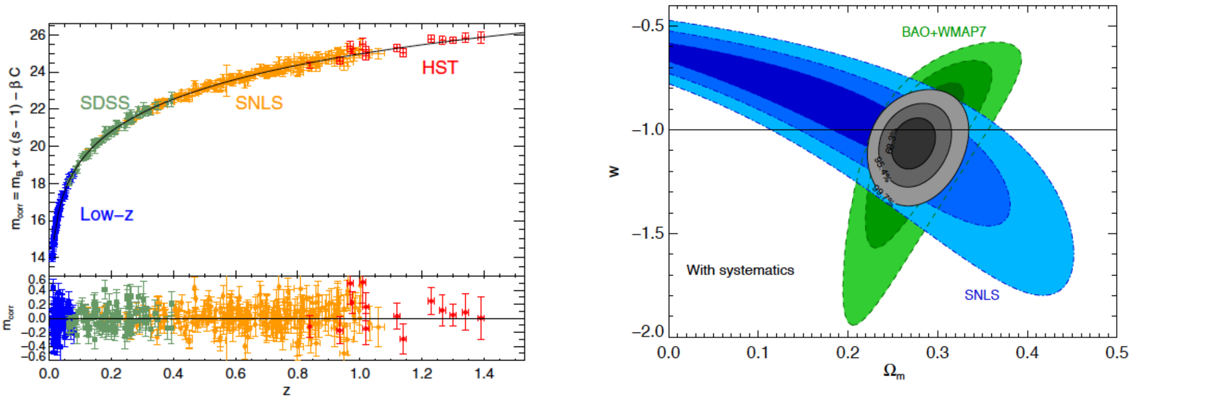

Fig. 1. Left: The Hubble diagram of SNe Ia (Conley et al. 2011). **Right:** Contours in the $w-\Omega_M$ plane. The blue areas are 68, 95 and 99% confidence level contrains from SNLS. The green areas show the constrains from baryon acoustic oscillations BAO/DR7 and WMAP7. The combined contours are shown in grey (Sullivan et al. 2011).

5 Conclusion

We have used the 3 year SNLS supernova sample along with nearby, intermediate and high redshift external SNe Ia samples to constrain the cosmological parameters governing the universal expansion. The SNLS sample is the largest, highest-quality of moderate to high redshift SN Ia sample. From SNe Ia samples only, we obtain w at a precision of 0.1 for a flat universe given a Ω_M measurement. Combining the supernova data with external probes (BAO and WMAP7), we obtain, for a flat universe, a precision of 5.5% on w (stat. only) increasing to $\sim 6.5\%$ if we include systematics. Refinements in the future will include a joint analysis of the 5 years of SNLS (~ 500 SNe Ia) with SDSS (~ 300 SNe Ia), taking full advantage of inter-calibration possibilities between the two experiments.

References

Astier, P., Guy, J., Regnault, N., et al. 2006, A&A, 447, 31
Balland, C., Baumont, S., Basa, S., et al. 2009, A&A, 507, 85
Baumont, S., Balland, C., Astier, P., et al. 2008, A&A, 491, 567
Conley, A., Guy, J., Sullivan, M., et al. 2011, ApJS, 192, 1
Ellis, R. S., Sullivan, M., Nugent, P. E., et al. 2008, ApJ, 674, 51
Guy, J., Astier, P., Baumont, S., et al. 2007, A&A, 466, 11
Guy, J., Sullivan, M., Conley, A., et al. 2010, A&A, 523, A7
Kessler, R., Becker, A. C., Cinabro, D., et al. 2009, ApJS, 185, 32
Kowalski, M., Rubin, D., Aldering, G., et al. 2008, ApJ, 686, 749
Regnault, N., Conley, A., Guy, J., et al. 2009, A&A, 506, 999
Sullivan, M., Conley, A., Howell, D. A., et al. 2010, MNRAS, 406, 782
Sullivan, M., Ellis, R. S., Howell, D. A., et al. 2009, ApJ, 693, L76
Sullivan, M., Guy, J., Conley, A., et al. 2011, ApJ, 737, 102
Sullivan, M., Le Borgne, D., Pritchet, C. J., et al. 2006, ApJ, 648, 868